




RESEARCH PAPER

# Funicular glass bridge prototype: design optimization, fabrication, and assembly challenges

Yao Lu · Alireza Seyedahmadian ·  
Philipp Amir Chhadeh · Matthew Cregan ·  
Mohammad Bolhassani · Jens Schneider ·  
Joseph Robert Yost · Gareth Brennan ·  
Masoud Akbarzadeh 

Received: 28 February 2022 / Accepted: 21 April 2022

© The Author(s), under exclusive licence to Springer Nature Switzerland AG 2022

**Abstract** Polyhedral Graphic Statics (PGS) is an effective tool for form-finding and constructing complex yet efficient spatial funicular structures. The intrinsic planarity of polyhedral geometries can be leveraged for efficient fabrication and construction using flat sheet materials, such as glass. Our previous research used PGS for the form-finding of a 3 m-span, modular glass bridge prototype to be built with thirteen unique hollow glass units (HGUs) in a compression-only configuration. This paper reports its design optimization, fabrication, and subsequent modular assembly process. The computational modeling of the

geometries is facilitated with the efficient half-face data structure provided by PolyFrame, a software that implements PGS. Regular float glass and acrylic are selected as the main structural materials, and they are fabricated using 5-axis water jet cutting and CNC milling techniques. With the help of 3 M™ Very High Bond tape, the glass parts and acrylic parts are bonded as HGUs, which serve as the basic structural and assembly modules. Surlyn sheets are used as interface material to prevent glass-to-glass direct contact between HGUs. The digital model is also simulated using ANSYS to ensure the effectiveness of the design. Due to the lightweight of the HGUs, the assembly of the bridge can be done by one person without the requirement of any heavy construction machinery.

**Keywords** 5-Axis water jet · 5-Axis CNC milling · Hollow glass unit · Funicular structure · Modular assembly

Y. Lu · M. Akbarzadeh (✉)  
Polyhedral Structures Laboratory, Department of  
Architecture, Weitzman School of Design, University of  
Pennsylvania, Philadelphia, PA, USA  
e-mail: masouda@upenn.edu

A. Seyedahmadian · G. Brennan  
Eventscape NY, New York, NY, USA

P. A. Chhadeh · J. Schneider  
Institute of Structural Mechanics and Design, Technische  
Universität Darmstadt, Darmstadt, Germany

M. Cregan · J. R. Yost  
Department of Civil and Environmental Engineering,  
Villanova University, Villanova, PA, USA

M. Bolhassani  
The Bernard and Anne Spitzer School of Architecture, The  
City College of New York, New York, NY, USA

M. Akbarzadeh  
General Robotic, Automation, Sensing and Perception (GRASP)  
Lab, School of Engineering and Applied Science, University of  
Pennsylvania, Philadelphia, PA, USA

## 1 Introduction

Many architects and engineers have studied and practiced graphical structural design methods based on 2D reciprocal diagrams during the past centuries for the generation of efficient structural forms (Cremona 1890; Culmann 1866; Maxwell 1864; Rankine 1864). The recent development of 3D graphic statics using polyhedral reciprocal diagrams, usually named as Polyhedral Graphic Statics (PGS), allows designers to

move beyond 2D and deal with complex spatial forms while being aware of the internal force distribution (Akbarzadeh 2016). One important feature that comes with PGS is the intrinsic planarity of the polyhedral geometries, which can be exploited for efficient fabrication and construction using flat sheet materials.

Flat sheet materials have certain advantages over other material types in building complex spatial forms due to their accessibility, processability, relatively low cost, and applicability in large scales (Akbari et al. 2021). More importantly, as a structural material, flat-sheet-based systems provide more load paths and consequently increase the stability under a wider range of loading cases compared to the traditional bar-node spatial framework. Flat glass sheets, for instance, have gained more attention in recent decades. However, the majority of the outstanding glass projects use it for architectural functionality purposes such as enclosing and daylighting, where the glass elements are structurally nonessential and are only responsible for out-of-plane wind or snow loads (Yost et al. 2022a). There is only a very limited number of architectural projects that use flat glass sheets for primary in-plane load-bearing purposes, for example, some Apple stores engineered by Eckersley O'Callaghan (O'Callaghan and Bostick 2012; O'Callaghan and Coult 2012).

Our previous research explores the in-plane strength of glass and aims to integrate the architectural functions with its structural potentials through hollow glass units (HGUs). The result shows that the individual HGU strength is governed by simultaneous flexural buckling of the deck plates at force levels well in excess of that required for the system strength (Yost et al. 2022a). A 10 m-span double-layer conceptual glass bridge design shows the feasibility of using the system of HGUs for modular and prefabricated construction approaches (Akbarzadeh et al. 2019). Later, the design and test fabrication of a 3 m-span reduced-scale bridge prototype that contains thirteen unique HGUs were presented to address the larger bridge's challenges regarding form-finding, detail developments, fabrication constraints, and assembly logic (Lu et al. 2021). Built upon all previous research, this paper reports a completed 3 m-span glass bridge prototype and its design optimization, fabrication, and assembly. This structure can be seen in assembled form in Fig. 1.

## 2 Form-finding and optimization

With the help of PolyFrame (Nejur and Akbarzadeh 2021; Nejur and Akbarzadeh 2018), a Rhino (Robert McNeel & Associates) plug-in that implements PGS, the form-finding can be achieved through two steps. The first step is creating a force diagram and its dual, form diagram. The generation of the force diagram starts from a 2D aggregation of polygonal faces, which defines the topology and load distribution of the bridge (Fig. 2a). By extruding this set of faces to a point, a set of 3D force polyhedrons is created. The extrusion height affects the rise and internal force distribution of the resulting single-layer funicular form diagram (Fig. 2b). Then, a double-layer bridge form diagram with thirteen closed polyhedron cells is derived by subdividing the force polyhedrons of the single-layer form diagram (Fig. 2c), and each closed cell is later materialized as one HGU.

The generation of the basic double-layer bridge form is followed by optimizing the global dimension, individual edge lengths, and face angles, which is to better satisfy the fabrication constraints and increase the ease of the subsequent fabrication process. The global dimension and individual edge lengths can be modified by setting vertex and edge length constraints. For the face angles, thanks to the reciprocal relationship between the force diagram and form diagram in PGS, the adjustment can be easily achieved by tuning the angles of their dual elements in its force diagram such that the planarity and equilibrium can be preserved. As a result of the adjustments of the edge lengths, the bridge dimension is set to 3.2 m(L)  $\times$  1.3 m(W)  $\times$  0.55 m(H), the thickness of the cells is set to around 100 mm, and each cell is constrained to a size that one person can handle during the construction process. Moreover, the orientations of the faces are carefully tuned such that all cells are self-interlocked under gravity.

## 3 Materialization strategy and fabrication

After having the base geometry of the bridge, the HGU details, and the steel abutments that hold all HGUs are devised based on the material selection and fabrication constraints. The geometries of all the parts are computationally modeled with the assistance of the handy geometrical data managing framework of PolyFrame

**Fig. 1** The completed 3 m glass bridge prototype

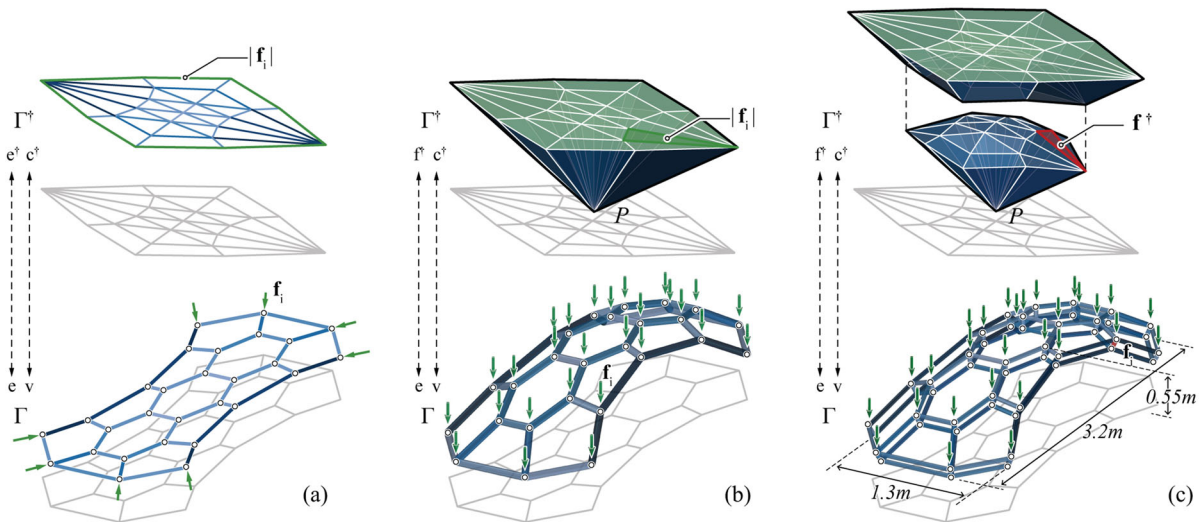


**Fig. 2** The form-finding process. **a** The 2D aggregation of polygons as force diagram and its reciprocal 2D form diagram; **b** the extruded polyhedrons as force diagram and its reciprocal 3D single-layer form diagram; **c** the further subdivided polyhedrons as force diagram and its reciprocal 3D double-layer form diagram

(Nejur and Akbarzadeh 2021) which follows the general rules of the half-face data structure (Kremer et al. 2013).

### 3.1 The hybrid data structure of PolyFrame

As mentioned earlier, each closed cell in the form diagram is materialized as one HGU. The hybrid data structure of PolyFrame provides all the basic geometric information required to generate intricate details. A pair of 3D reciprocal diagrams in the context of PGS consists of one force diagram and one form diagram that are geometrically dependent and topologically dual. They

are almost identical in terms of the organization of data which has 4 levels: vertices, edges, faces, cells. Vertices store the geometrical information of coordinates, while the edges, faces, and cells define the topology (Fig. 3a). The only difference between form and force diagrams is that the form diagram usually contains both open and closed polyhedral cells, while force diagrams usually only have closed cells, and the edge of the open cells in the form diagram represents the external forces. In this section, the description and explanation only focus on the form diagram which the computational modeling relies on.

Since the geometry and topology are thoroughly described by the vertices, edges, faces, and cells, almost

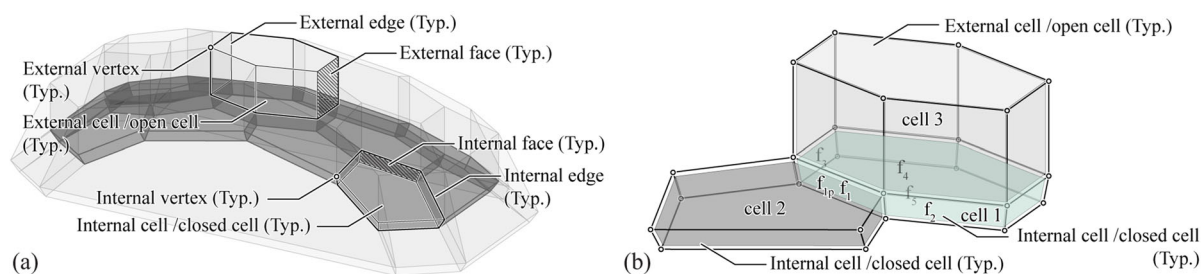


**Fig. 3** **a** The form diagram of the glass bridge that shows the four levels of geometrical and topological information, and only internal cells will be materialized as HGUs; **b** The geometrical information of face  $f_1$  such as area, centroid, and plane can be computed based on its four corner coordinates. The topological information can also be easily queried, such as face pair ( $f_{1p}$ ), all connected faces in the same cell ( $f_2, f_3, f_4, f_5$ )

all the geometric information and relationships can be easily queried from the data structure. For any face in the form diagram (Fig. 3b), the area, centroid, and plane of it can be computed based on the coordinates of its corner vertices. Moreover, it is easy to find its paired face and all connected faces while knowing which cell each face belongs to and whether the cell is closed or open. Built upon those basic queries of geometric information, more complex geometric operations can be done.

### 3.2 Hollow glass unit (HGU)

As the basic construction module, each individual HGU needs to have sufficient strength along the load path, and also be able to accommodate the connection details with its neighbors, so the details are designed accordingly. Each of the thirteen closed polyhedron cells has a top and a bottom face, and several smaller side faces. The two top and bottom faces are the largest and all other smaller faces are side faces, so they can be easily distinguished from the data structure when sorted by area.

Each of the two top and bottom faces is materialized as a glass deck plate using 9.5 mm annealed glass. For the smaller side faces, they are materialized as either 9.5 mm-thick glass side plates or 21 mm-thick acrylic side plates depending on whether they need to accommodate the connection mechanisms with the neighbor HGUs (Fig. 4a). The connection mechanism between neighboring HGUs contains two pocket channels on the pair of facing side plates and a locking strip that has a butterfly shape section profile. This butterfly

connection mechanism is improved from the male–female locking mechanism proposed for our previous round of test fabrication (Lu et al. 2021), and it better prevents most relative movements of the neighboring HGUs and safeguards against extreme loads (more details of the butterfly connection mechanism are discussed in Sect. 3.4). For each face that does not face a closed neighbor cell, meaning it's a “naked face” that is not between two HGU and hence doesn't need to have the butterfly connection mechanism, it is materialized as a glass side plate using 9.5 mm annealed glass. For the other side faces that are attached to a closed neighbor cell, they are materialized as 21 mm-thick acrylic side plates. Glass is not used for those side plates because the fabrication of irregular glass shapes is costly and there is difficulty providing the required precision (Lu et al. 2021). All the glass plates are cut using 5-axis abrasive water jet cutter, and the acrylic plates are milled using 5-axis milling machines. After cutting is complete, all glass and acrylic plates of an individual HGU are bonded together using 3 M™ Very High Bond (VHB) transparent structural tape, a type of double-sided soft bonding agent (Fig. 4b). In the fully assembled bridge, all the top and bottom glass deck plates form two continuous layers and serve as the primary load transfer elements (Fig. 5).

With the basic geometrical information in the data structure, the geometries of all the deck plates and side plates can be sculptured by their boundary planes as illustrated in Fig. 6a. For example, to generate one typical top deck plate, the first step is taking the plane of its corresponding face. Then the plane is duplicated and offset towards inside the cell by the thickness of the deck plate, which is 9.5 mm. The offset plane and the



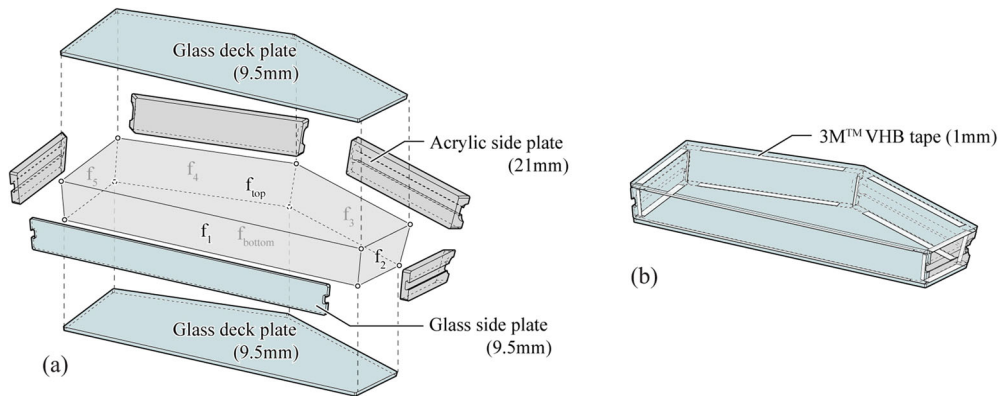


**Fig. 4** A typical closed cell is materialized as an HGU. **a** The top face  $f_{top}$  and bottom face  $f_{bottom}$  are materialized as deck plates; the “naked” side face  $f_1$  is materialized as a glass side plate; all other faces are materialized as acrylic side plates; **b** All deck plates and side plates are bonded with 3 M™ VHB tape

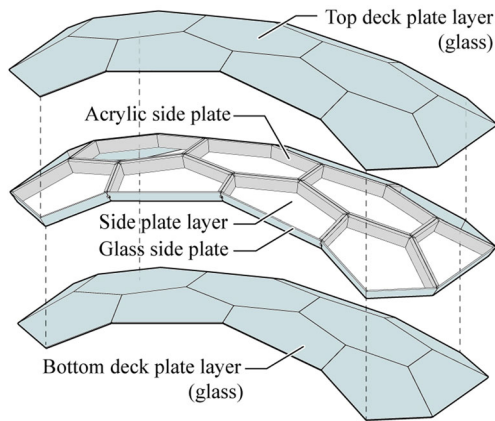


**Fig. 5** The top and bottom deck plates form two continuous layers and serve as the primary load transfer elements

original plane define the internal and external boundaries of the deck plate. Then, the planes of all the side faces are taken out to help generate the cutting perimeters. Those side planes may need to be offset inwards to leave space for the Surlyn sheet interface between this deck plate and the deck plate from the neighboring cells (the interface materials will be described with more details in Sect. 3.5). Offset only happens when the face is sitting between two closed cells, meaning that there needs to be a Surlyn sheet interface. The offset distance is half of the interface thickness, which is about 1.6 mm. The other half of the required space

will be given by the same operation from the neighboring cell. Later, all the planes mentioned above are used to generate a boundary volume, which represents the geometry of the deck plate. Lastly, the sharp corners are rounded using 5 mm radius fillet. The 5-axis abrasive water jet cutter has a maximum cutting angle of 59 degrees from vertical. The cutting angles of the deck plate can be computed as the tilting angles of the side planes relative to the top plane, and they are all ensured below the maximum cutting limit.

The geometries of the side plates are generated using similar plane operations as illustrated in Fig. 6b. Take for example a typical acrylic side plate, the plane of its corresponding face is first taken and offset towards the inside of the cell to leave space for the interface material (i.e. Surlyn). Thereafter, this plane is duplicated and offset again by the thickness of acrylic, which is 21 mm. Those two planes define the internal and external boundaries of the side plate. Then, another four planes are required to define the other boundaries. The first two planes are derived from offsetting the top and bottom planes inwards by the summation of deck plate thickness (9.5 mm) and VHB tape thickness (1 mm), which determines the boundaries that face the two deck plates. The other two planes that define the boundaries facing the adjacent side plates are more complex as it also depends on the type of the connected side faces. If a connected side face is a “naked face”, meaning that the boundary faces to a glass side plate, then the plane is obtained through offsetting the plane of that connected face by the summation of glass side plate thickness

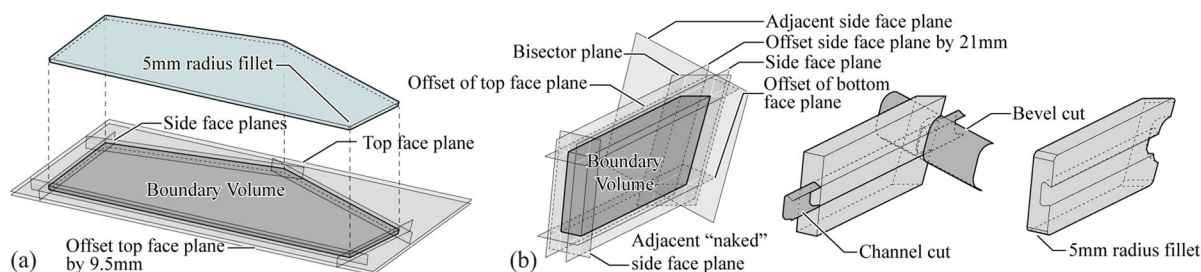


**Fig. 6** The geometries of deck plates and side plates are generated using planes. **a** The generation of a typical glass deck plate; **b** the generation of a typical acrylic side plate

(9.5 mm) and VHB tape thickness (1 mm). Otherwise, meaning that the boundary faces to an acrylic side plate, the bisector plane of the two side faces is computed first as the middle plane, then this plane is offset by half of the VHB tape thickness (the other half will be provided by the same operation when generating the model of the other acrylic side plate). Up to this point, all 6 boundary planes are computed, and a boundary volume is generated. Like the deck plates, all sharp corners are rounded with 5 mm radius fillet. Finally, the pocket channel is carved out from the acrylic side plates using a predefined butterfly profile. The generation of the glass side plate geometries is similar to the acrylic side plates but simpler, so it's omitted from the description. The glass side plates are cut using 5-axis water jet cutting, and again, the cutting angles are informed by manufacturing and assembly constraints. The acrylic side plates are made using 5-axis CNC router.

### 3.3 Steel abutment supports

All thirteen HGUs are restrained by a pair of steel abutments made of 9.5 mm steel sheets (Figs. 1, 8b). All parts of the abutments are cut into shapes using a 3-axis industrial laser cutter and then manually welded together. The laser cutter has an accuracy of less than  $\pm 0.01$  mm, however, locating those parts and the manual welding process is prone to a much larger error. In order to ensure precision, the parts of the abutments are designed to be self-locating by incorporating tabs and slots that can be accurately cut with the laser cutter.

To counteract the thrust generated by the bridge, the pair of abutments are connected by tension ties that are made of off-the-shelf steel products such as turnbuckles and threaded rods. The abutments also have bolt holes

so they can be bolted onto a laboratory strong floor for heavier loads and future testing purposes.

### 3.4 Butterfly locking mechanism

As mentioned earlier, each butterfly locking mechanism consists of two parts: the two pocket channels on the side plates of the pair of HGUs to be connected, and a locking strip flip-milled out of acrylic. The strips can be inserted from the end of the channels (Figs. 7, 8a), however, it's important to note that since a strip can only be inserted when the channel has at least one end that is not occluded, certain side plates cannot have the butterfly locking mechanism because both ends of the channel are blocked by either the neighboring HGUs or the steel abutments (Fig. 8b). The locations of those side plates are highly dependent on the HGU assembly sequence, and it will be further discussed in Sect. 5.2. The profile of the pocket channels and locking strips is determined by the shape and size of the tool bits such that the 5-axis CNC milling can be achieved with shorter tool paths. On the interface of the pockets and locking strip, a tolerance of 0.2 mm is left. To make disassembly possible, a bevel and a hole are cut at one end of each locking strip such that they can be taken out with a hook (Fig. 7).

### 3.5 Interface material

Direct contact between glass deck plates of neighboring HGUs, and glass with any other hard material (such as steel at the abutments) should be strictly avoided as it causes stress concentration and cracking of the glass parts. Therefore, soft substances are placed between every glass-to-glass, glass-to-steel, and glass-to-acrylic



**Fig. 7** A locking strip is inserted into the channels of two neighboring HGUs

contact. Within each HGU, VHB tape serve as the soft insulation material, which comes as an off-the-shelf product and can be easily trimmed to shapes by a knife. Between the neighboring HGU deck plates and between the HGUs and steel abutments, Surlyn sheets cut with a 3-axis CNC router are placed (Fig. 8a) and used as the interface material preventing direct glass-to-glass, and glass-to-steel contact.

#### 4.4. Structural analysis

Before HGU fabrication and bridge assembly, a static numerical finite element analysis is conducted using ANSYS, which follows the previously established analysis sequence as explained by Yost et al. (2022a). The major purpose of the numerical analysis is to examine the performance of the butterfly locking mechanisms and the behavior of the bridge under dead load, and hence ensure the validity and integrity of the proposed modular glass bridge design.

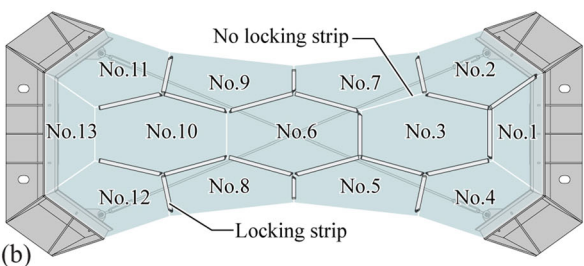
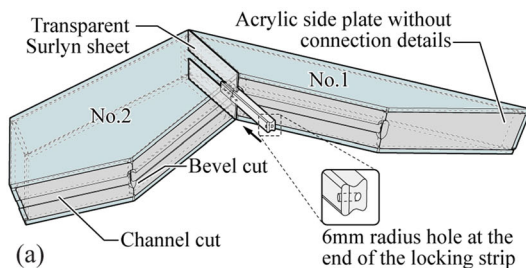


**Fig. 8** **a** A typical connection between two HGUs; **b** Assembly sequence and corresponding locations of the locking strips

For the butterfly locking mechanism, two simplified bridge models with 2 HGUs are devised to carry out a comparative study, one with flat side plates (Fig. 9a, b) and another with a butterfly locking mechanism (Fig. 9c, d). Two loading scenarios are simulated for each model, one with dead load and 1kN along the negative-Z direction applied to the two adjacent edges of the HGUs (Fig. 9a, c), another with the same dead load but 1kN along the positive-Z direction (Fig. 9b, d). Contacts between the acrylic elements and the Surlyn plates are friction-based with a coefficient of 0.2, the same as that between Surlyn and the deck plates. This is intentionally low to accommodate for marginal gaps on contacting surfaces or other imperfections in the real construction. Contacts between VHB tape and glass plates, VHB tape and acrylic side plates are set to surface-to-surface bonded contact. The model emitted the steel abutments that support the HGUs for simplicity. Instead, it is pin supported at the Surlyn plates at the two ends of the bridge which functions as an inter-layer between the HGUs and the steel support structure. The material parameters for Surlyn are obtained from the physical experiments done at Villanova (Yost et al. 2022b).

The analytical model investigates how the butterfly locking mechanism affects HGU displacements under two extreme cases. The directional deformation along the Z direction is recorded. It is clearly seen in Fig. 9a that the left HGU slides down due to lack of connection at the HGU interface. It's more apparent in Fig. 9b that the contact is lost due to the uplifting force, and consequently ANSYS fails to complete the simulation because of the sudden change of the contact pairs. In contrast, Fig. 9c, d show that the structure can withstand both loading scenarios with the maximum deformation of 0.61 mm and 3 mm for -Z and +Z directed

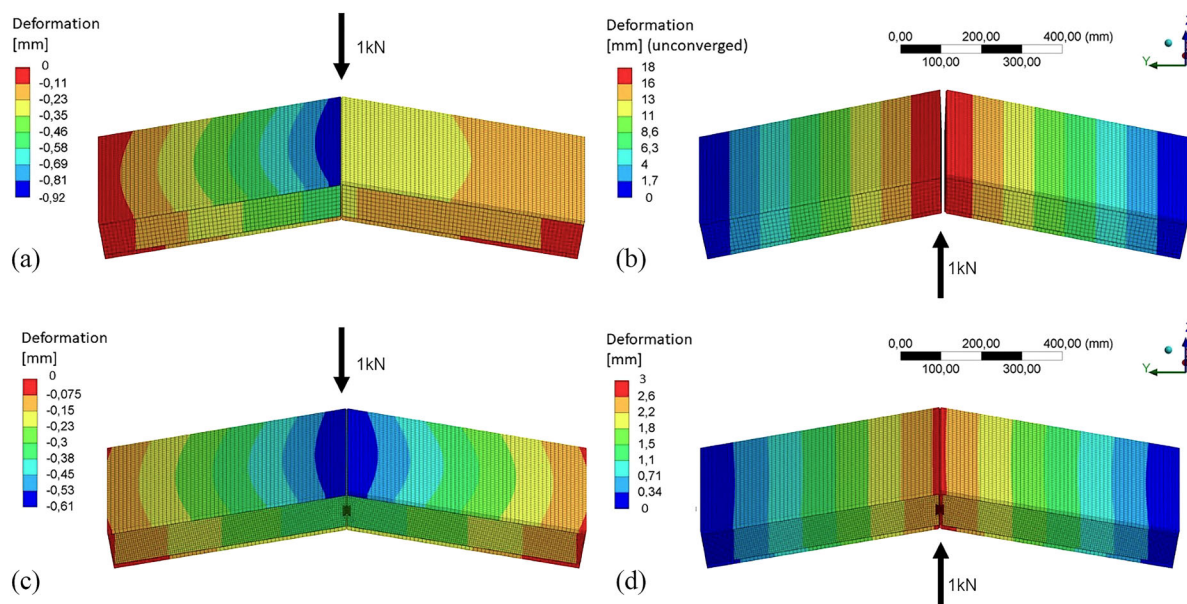


**Fig. 9** A comparative study using two simplified bridge models to examine the behavior of the butterfly locking mechanism. **a, b** only have flat side plates and serve as the control group, while **c, d** has the butterfly connection mechanism. **a, c** are loaded with self-weight and 1kN along the negative-Z direction, and **b, d** are loaded with self-weight and 1kN along the positive-Z direction

forces, respectively. This indicates that the butterfly locking mechanism successfully improves the performance. It's also important to note that the model is not able to simulate glass cracking and it needs to be checked manually for each result.

Finally, the same setup is used to simulate the whole bridge (Fig. 10). The result shows that the bridge can sustain its self-weight. More comprehensive simulations of different load cases will follow in future investigations to fully understand the performance of the bridge.

## 5 Assembly

The assembly process consists first of the assembly of the individual HGUs followed by assembly of the entire bridge. The heaviest HGU of the bridge weighs about 23.3 kg (No.10 in Fig. 8b), meaning that the assembly process can be handled by one person without any heavy construction machinery. Moreover, most material can be easily dismantled and recycled at the end of its life cycle as a consequence of the dry assembly process.

### 5.1 Assembly of a Typical HGU

Both CNC milling and 5-axis water jet cutting provide a good fabrication accuracy for the individual parts. Then, some jigs and bars are developed to help facilitate the assembly of each HGU and locate the parts before permanently bonding them with VHB tape. The jigs are 3d-printed with polylactic acid (PLA), and the bars are CNC cut from 6 mm high-density polyethylene (HDPE) sheets.

The jigs and bars work together as hoops, which confine the angles of the individual parts and the overall dimensions of the HGUs. The assembly of a typical HGU is illustrated in Figs. 11 and 12. First, the bonding areas of all glass and acrylic parts are cleaned using isopropyl alcohol, and this is followed by priming using 3 M™ Silane Glass Treatment AP115 to improve bond performance. Then, the jigs are placed at the corners of the smaller bottom deck plate of the two. Next, the jigs are connected by the HDPE bars hence one hoop is completed, which confines the precise positions of the acrylic side plates (Figs. 11a, 12a). Before placing the side plates onto the deck plate, they are first connected into a side-wall loop using VHB tape (Fig. 12b). VHB tape is also applied to the bottom surface of the side wall



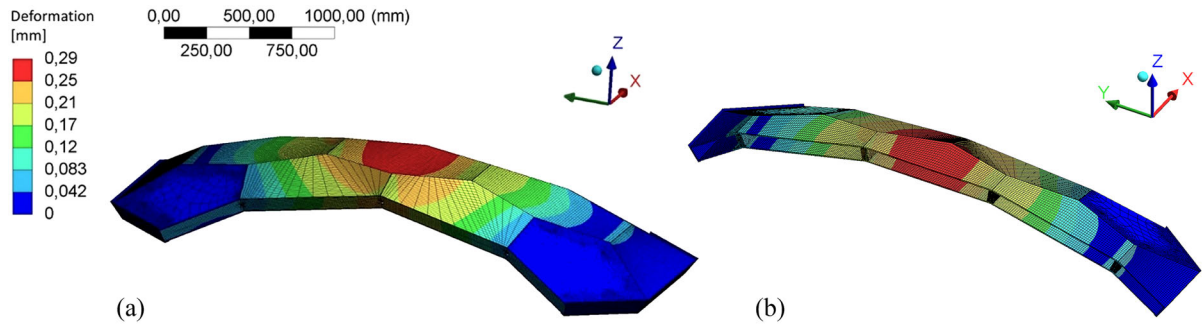
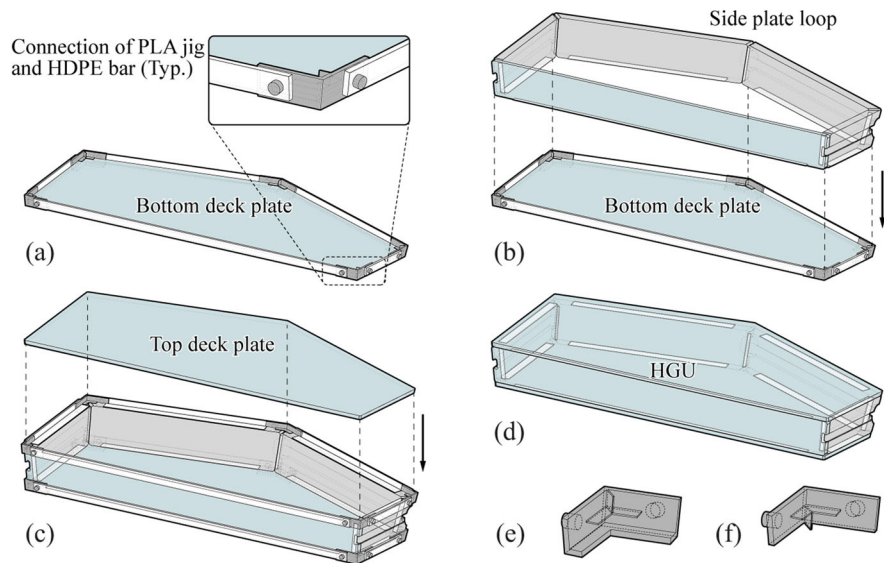


**Fig. 10** **a** The finite element model of the bridge under dead load with the total Deformation color-coded in [mm]. **b** The section view of the finite element model

**Fig. 11** **a** The bottom deck plate and the bottom hoop of PLA jigs and HDPE bars; **b** all side plates are connected into a side-wall loop, then bonded to the bottom deck plate; **c** place the top hoop of PLA jigs and HDPE bars, and place the top deck plate into the hoop; **d** remove all PLA jigs and HDPE bars; **e** a typical bottom jig; **f** a typical top jig



loop (Fig. 12c), and the whole loop is moved onto the smaller deck plate with its position trued by the hoop (Figs. 11b, 12d). At this point, the smaller bottom deck plate and all the side plates are bonded together.

This is followed by the placement of the larger top deck plate. First, VHB tape is applied to the top surface of the side-wall loop. Next, the jigs are put onto the top corners of the side-wall loop and connected into a second hoop using HDPE bars, which confines the position of the larger top deck plate (Fig. 12e). Then, the top deck plate is put into the second hoop, and therefore all deck plates and side plates are bonded together (Figs. 11c, 12f). To strengthen the bonding of the VHB tape, clamps are used to apply a recommended pressure of about 100 kPa (Fig. 12g). Lastly, all PLA jigs and HDPE bars are removed from the assembly (Fig. 12h) completing the assembly of one HGU (Figs. 11d, 12i).

## 5.2 Assembly of the bridge

Assembly of the whole bridge begins only after assembly of all thirteen HGUs is completed. Bridge assembly starts with placing some CNC-cut plywood panels on the floor to locate the two steel abutments precisely. Then, the two steel abutments are put on the floor and attached to the plywood panels with shims underneath for leveling purposes. After the locations of the steel abutments are precisely found, two tension ties are connected to the abutments and tightened for stability. The tension ties will also be key structural elements because they counteract the thrusts created by the HGUs and ensure a compression dominant state within the bridge (Fig. 13a).

The height-adjustable falsework is then placed on the plywood panels (Fig. 13b). This falsework consists

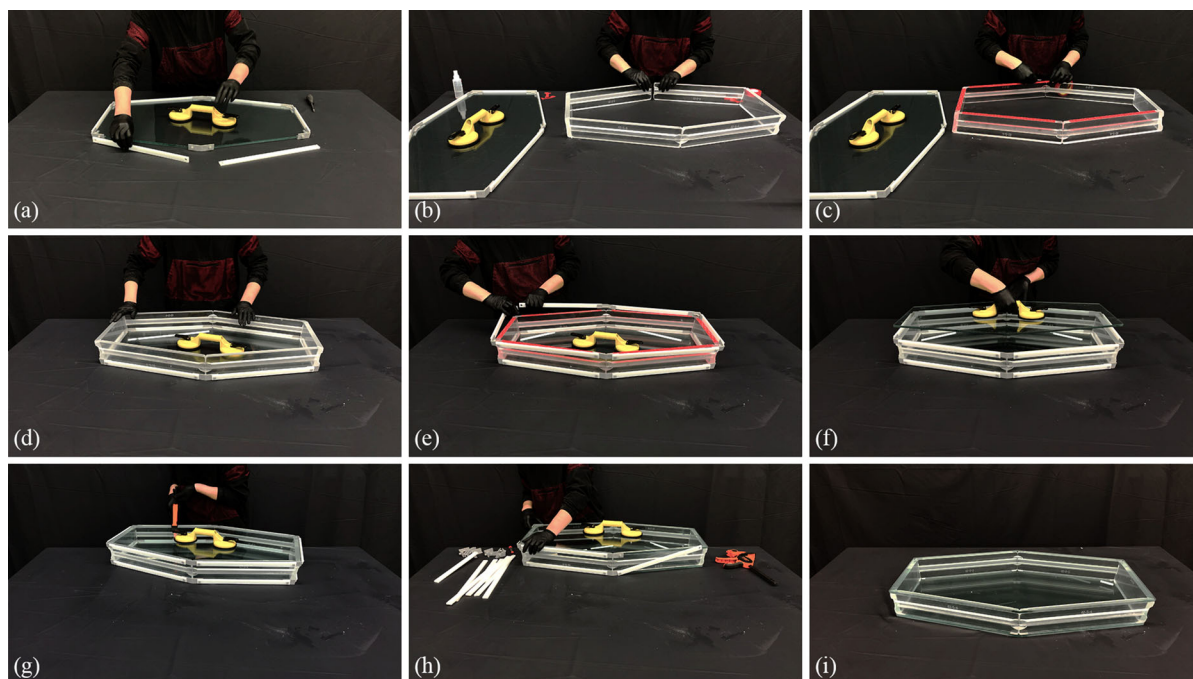


**Fig. 12** Photos of the assembly of a typical HGU. **a** The bottom deck plate and the bottom hoop of PLA jigs and HDPE bars; **b** all side plates are connected into a side-wall loop; **c** apply VHB tape to the bottom of the side-wall loop; **d** bond the side-wall loop to the bottom deck plate; **e** apply VHB tape to the top of the side-wall loop and place the top hoop of PLA jigs and HDPE bars; **f** place the top deck plate into the hoop; **g** strengthen the VHB bonding using a clamp; **h** remove all PLA jigs and HDPE bars; **i** a completed HGU

of plywood waffle structures and leveling feet that have an adjustable range of 7 cm. It is designed into two separate parts each having three layers such that it can be easily taken apart and removed from below the bridge after the assembly is done. The Surlyn sheets are later placed on the steel abutments to avoid steel-to-glass contact. For other Surlyn sheets between the HGUs, one side of each sheet is glued to the corresponding HGU to fix its position using Gorilla™ transparent spray adhesive, which provides strong bonds without adding much construction error. However, one disadvantage of the spray adhesive is that the adhesive particles damage the transparency of the Surlyn sheet and as a result, the interface areas become foggy. To avoid this issue, the adhesive is only sprayed to a narrow edge area that contacts the edge of the deck plate, leaving the majority of the Surlyn sheet untouched. It turns out that this narrow area of spray adhesive can provide adequate bonding.

As mentioned earlier, the choice of the assembly sequence of HGUs has a large impact on the count and locations of butterfly locking connections. It is also critical to note that the final “keystone” HGU may not have any butterfly locking mechanism on its side plates

and hence it is more vulnerable to sliding and rotation. For this reason, a unit directly supported by the steel abutment with four sides is selected as the “keystone” (Fig. 8b, unit No. 13). The final assembly sequence is selected aiming for the least number of side plate pairs that cannot have butterfly connection, and eventually, twenty out of the total twenty-six HGU-to-HGU contacts are secured by the butterfly locking mechanisms. Construction errors are almost inevitable at such scales, and it’s impossible to know how the errors would build up in advance. In the construction of the Armadillo Vault by Block Research Group (BRG), the final keystones were not pre-cut, and they were cut only when all the other stones are in place and the space left is measured to ensure the perfect fit (Block et al. 2018). The distance between the two steel abutments can be tuned by the turnbuckle to accommodate some errors in the glass bridge assembly. Also, the ductility of the Surlyn sheets helps take a certain level of errors.

The decentering process starts after the last HGU has been put into place. An Allen wrench is used to adjust the leveling feet and lower the falsework (Fig. 13e). In each round of adjustment, all eight leveling feet are

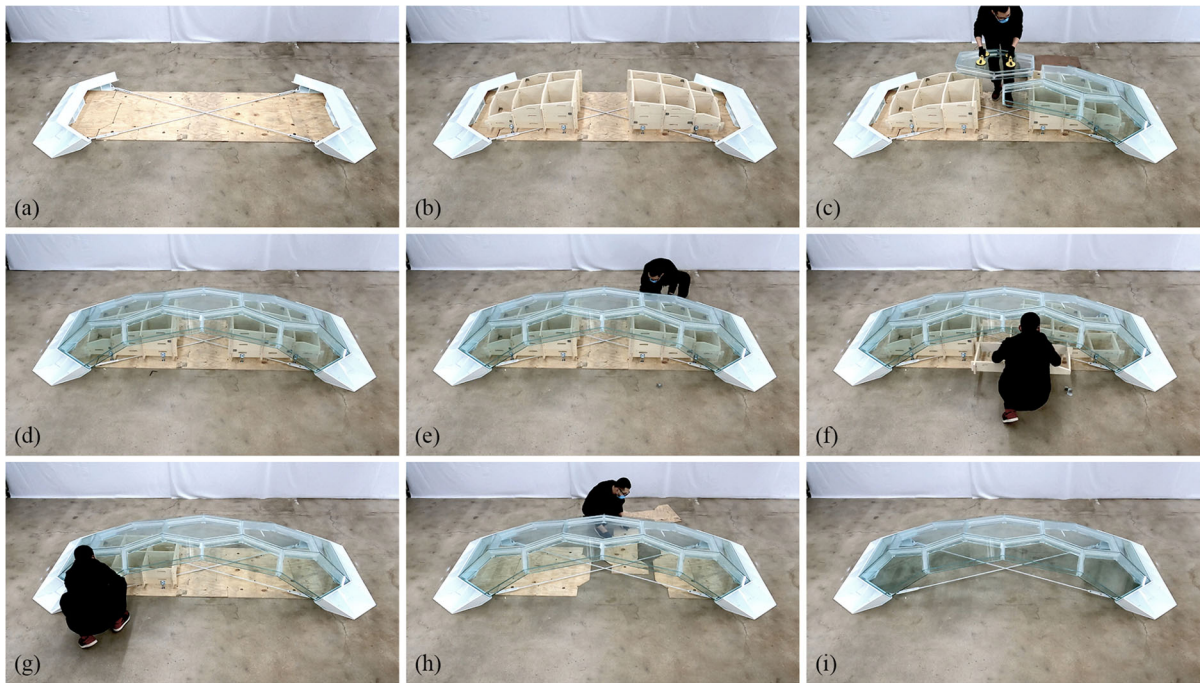
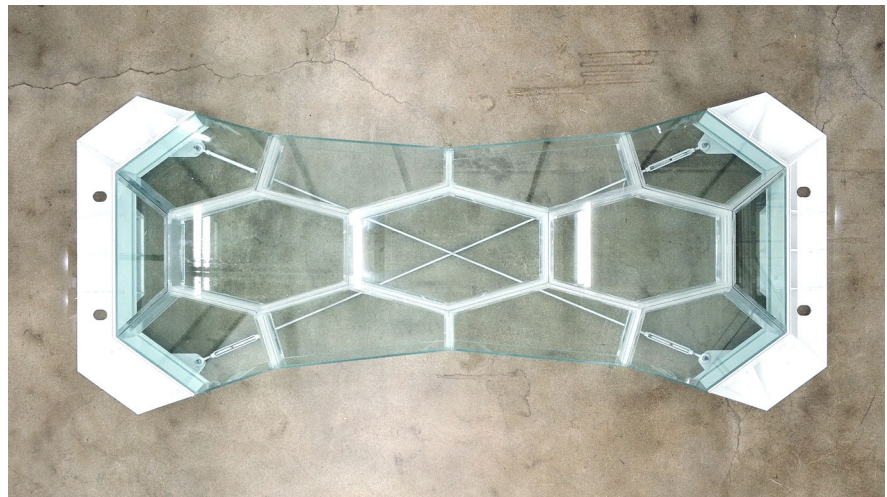


**Fig. 13** **a** Use plywood panels to locate the steel abutments; **b** place the falsework on the plywood panels; **c, d** put HGUs on the falsework; **e** turn the leveling feet and lower the falsework; **f** remove the middle layer of the falsework; **g** remove the other parts of the falsework; **h** remove the plywood panels; **i** completed glass bridge

**Fig. 14** Top view of the assembled bridge prototype



rotated by half a turn and the falsework is lowered by around 0.75 mm. After several rounds, the falsework is fully detached from the HGUs, showing that the self-weight of the bridge has been transferred to the steel abutments through the HGUs. Each part of the falsework is then dismantled into 3 separate layers otherwise the opening under the bridge does not allow the

falsework to come out as a whole (Fig. 13f, g). The middle layer is taken out first, the top layer follows, and the bottom layer is removed last. Finally, the plywood panels are removed from the floor, marking the end of the assembly (Fig. 13h, i). Figure 14 shows the top view of the assembled bridge. In the near future, physical experiments will be conducted to fully explore



the structural performance of the 3 m-span bridge. As well, the experimental results will be used to calibrate an ANSYS model to improve numerical reliability in predicting the response of this 3 m-span bridge, and other structural systems constructed from the assembly of the individual HGUs.

## 6 Conclusion

This paper presents the computational design, optimization, fabrication, and assembly process of a three-meter glass bridge prototype that uses HGUs as construction modules. It shows that PGS can be exploited not only in the design of complex space frames but also in spatial plate-based structures. This paper also demonstrates that by the modular construction system of HGUs, 9.5 mm float glass, a brittle material in tension, can have considerable load-bearing potential and can be used as a structural material in creating complex spatial structures. The modular system is also proved to be lightweight so the entire construction process can be handled by one person. Moreover, the entire assembly is modular and can be easily disassembled and reconstructed at a different location. Currently, the glass bridge can sustain its own self-weight with negligible deformation. Its performance under other loading scenarios awaits future experimental studies.

**Acknowledgements** This research was supported by University of Pennsylvania Research Foundation Grant (URF), National Science Foundation CAREER AWARD (NSF CAREER-1944691- CMMI) and the National Science Foundation Future Eco Manufacturing Research Grant (NSF, FMRG-CMMI 2037097) to Dr. Masoud Akbarzadeh. Also, this study was supported by Villanova University Summer Grant Program (USG) to Dr. Joseph Yost. The multi-axis milling, metalwork, and other facilities were generously supported by Eventscape NY.

## Declarations

**Conflict of Interest** The authors have NO known affiliations with or involvement in any organization or entity with any financial interest, or non-financial interest in the subject matter or materials discussed in this manuscript.

## References

Akbari, M., Lu, Y., Akbarzadeh, M.: From design to the fabrication of shellular funicular structures. In: ACADIA 2021:

- REALIGNMENT—Towards Critical Computation (Proceedings of the 41st Annual Conference of the Association for Computer Aided Design in Architecture (ACADIA)) (2021). <https://par.nsf.gov/biblio/10314969>
- Akbarzadeh, M.: 3D Graphical Statics Using Reciprocal Polyhedral Diagrams (2016). <http://hdl.handle.net/20.500.11850/183500>
- Akbarzadeh, M., Bolhassani, M., Nejur, A., Yost, J.R., Byrnes, C., Schneider, J., Knaack, U., Costanzi, C.B.: The design of an ultra-transparent funicular glass structure. In: Structures Congress 2019, pp. 405–413. American Society of Civil Engineers, Orlando, Florida (2019)
- Block, P., Mele, T., Liew, A., DeJong, M., Escobedo, D., Ochsendorf, J.: Structural design, fabrication and construction of the Armadillo vault. *Struct. Eng.* **96**, 10–20 (2018)
- Cremona, L.: Graphical Statics. Two Treatises on the Graphical Calculus and Reciprocal Figures in Graphical Statics. Clarendon Press (1890)
- Culmann, C.: Die Graphische Statik. Meyer & Zeller (1866)
- Kremer, M., Bommers, D., Kobbelt, L.: OpenVolumeMesh—A Versatile Index-Based Data Structure for 3D Polytopal Complexes. In: Jiao, X., Weill, J.-C. (eds.) Proceedings of the 21st International Meshing Roundtable, pp. 531–548. Springer, Berlin (2013)
- Lu, Y., Cregan, M., Chhadeh, P., Seyedahmadian, A., Bolhassani, M., Schneider, J., Yost, J., Akbarzadeh, M.: All glass, compression-dominant polyhedral bridge prototype: form-finding and fabrication (2021)
- Maxwell, J.C.: On reciprocal figures and diagrams of forces. *Philos. Mag.* **27**, 250–261 (1864)
- Nejur, A., Akbarzadeh, M.: PolyFrame (2018)
- Nejur, A., Akbarzadeh, M.: PolyFrame, efficient computation for 3D graphic statics. *Comput.-Aided Des.* **134**, 1003 (2021)
- O’Callaghan, J., Bostick, C.: The apple glass cube: version 2.0. *Challeng. Glass* **3**, 57–65 (2012). <https://doi.org/10.3233/978-1-61499-061-1-57>
- O’Callaghan, J., Coult, G.: An All Glass Cube in New York City, pp. 1–6 (2012). [https://doi.org/10.1061/41016\(314\)74](https://doi.org/10.1061/41016(314)74)
- Rankine, W.J.M.: XVII. Principle of the equilibrium of polyhedral frames. *Lond. Edinb. Dublin Philos. Mag. J. Sci.* **27**, 92–92 (1864). <https://doi.org/10.1080/14786446408643629>
- Robert McNeel & Associates: Rhinoceros 3D.
- Yost, J.R., Bolhassani, M., Chhadeh, P.A., Ryan, L., Schneider, J., Akbarzadeh, M.: Mechanical performance of polyhedral hollow glass units under compression. *Eng. Struct.* **254**, 113730 (2022a). <https://doi.org/10.1016/j.engstruct.2021.113730>
- Yost, J. R., Cregan, M., Bolhassani, M., Akbarzadeh, M., Lu, Y., Chhadeh, P.A., & Schneider, J.: Experimental Investigation of a Transparent Interface Material for Glass Compression Members. Accepted conference paper manuscript for Challenging Glass Conference 8 (2022b)

**Publisher’s Note** Springer Nature remains neutral with regard to jurisdictional claims in published maps and institutional affiliations.